J|A|C|S
ARTICLES
Published on Web 12/08/2006

Calculation of Vibronic Couplings for Phenoxyl/Phenol and Benzyl/Toluene Self-Exchange Reactions: Implications for Proton-Coupled Electron Transfer Mechanisms

Jonathan H. Skone, Alexander V. Soudackov, and Sharon Hammes-Schiffer*

Contribution from the Department of Chemistry, 104 Chemistry Building, Pennsylvania State University, University Park, Pennsylvania 16802

Received August 14, 2006; E-mail: shs@chem.psu.edu

Abstract: The vibronic couplings for the phenoxyl/phenol and the benzyl/toluene self-exchange reactions are calculated with a semiclassical approach, in which all electrons and the transferring hydrogen nucleus are treated quantum mechanically. In this formulation, the vibronic coupling is the Hamiltonian matrix element between the reactant and product mixed electronic−proton vibrational wavefunctions. The magnitude of the vibronic coupling and its dependence on the proton donor−acceptor distance can significantly impact the rates and kinetic isotope effects, as well as the temperature dependences, of proton-coupled electron transfer reactions. Both of these self-exchange reactions are vibronically nonadiabatic with respect to a solvent environment at room temperature, but the proton tunneling is electronically nonadiabatic for the phenoxyl/phenol reaction and electronically adiabatic for the benzyl/toluene reaction. For the phenoxyl/phenol system, the electrons are unable to rearrange fast enough to follow the proton motion on the electronically adiabatic ground state, and the excited electronic state is involved in the reaction. For the benzyl/toluene system, the electrons can respond virtually instantaneously to the proton motion, and the proton moves on the electronically adiabatic ground state. For both systems, the vibronic coupling decreases exponentially with the proton donor−acceptor distance for the range of distances studied. When the transferring hydrogen is replaced with deuterium, the magnitude of the vibronic coupling decreases and the exponential decay with distance becomes faster. Previous studies designated the phenoxyl/phenol reaction as proton-coupled electron transfer and the benzyl/toluene reaction as hydrogen atom transfer. In addition to providing insights into the fundamental physical differences between these two types of reactions, the present analysis provides a new diagnostic for differentiating between the conventionally defined hydrogen atom transfer and proton-coupled electron transfer reactions.

I. Introduction

The coupling of electron and proton transfer reactions plays a vital role in a wide range of chemical and biological processes, including photosynthesis,[1−6] respiration,[7,8] and enzyme reactions.[9−13] A general term for reactions in which an electron and a proton are transferred in a single step is proton-coupled electron transfer (PCET). Traditionally, reactions in which the electron and proton transfer between the same donor and acceptor are denoted hydrogen atom transfer (HAT), and the term PCET is often reserved for reactions in which the electron and proton transfer between different donors and acceptors.[14−18] This distinction, however, is not rigorous because the electron and proton behave quantum mechanically. Nevertheless, understanding the fundamental differences between these two types of reactions is important for the study of many chemical and biological processes.

Recently, Mayer, Borden, and co-workers used density functional theory to investigate the self-exchange reactions of the phenoxyl radical with phenol and the benzyl radical with toluene.[14] These authors identified the former as a PCET reaction and the latter as an HAT reaction. This identification was based on an analysis of the singly occupied molecular orbital (SOMO)

(1) Babcock, G. T.; Barry, B. A.; Debus, R. J.; Hoganson, C. W.; Atamian, M.; McIntosh, L.; Sithole, I.; Yocum, C. F. *Biochemistry* **1989**, *28*, 9557−9565.
(2) Okamura, M. Y.; Feher, G. *Annu. Rev. Biochem.* **1992**, *61*, 861−896.
(3) Tommos, C.; Tang, X.-S.; Warncke, K.; Hoganson, C. W.; Styring, S.; McCracken, J.; Diner, B. A.; Babcock, G. T. *J. Am. Chem. Soc.* **1995**, *117*, 10325−10335.
(4) Hoganson, C. W.; Babcock, G. T. *Science* **1997**, *277*, 1953−1956.
(5) Hoganson, C. W.; Lydakis-Simantiris, N.; Tang, X.-S.; Tommos, C.; Warncke, K.; Babcock, G. T.; Diner, B. A.; McCracken, J.; Styring, S. *Photosynth. Res.* **1995**, *47*, 177−184.
(6) Blomberg, M. R. A.; Siegbahn, P. E. M.; Styring, S.; Babcock, G. T.; Akermark, B.; Korall, P. *J. Am. Chem. Soc.* **1997**, *119*, 8285−8292.
(7) Babcock, G. T.; Wikstrom, M. *Nature* **1992**, *356*, 301−309.
(8) Malmstrom, B. G. *Acc. Chem. Res.* **1993**, *26*, 332−338.
(9) Siegbahn, P. E. M.; Eriksson, L.; Himo, F.; Pavlov, M. *J. Phys. Chem. B* **1998**, *102*, 10622−10629.
(10) Blow, D. M. *Acc. Chem. Res.* **1976**, *9*, 145.
(11) Ramaswamy, S.; Eklund, H.; Plapp, B. V. *Biochemistry* **1994**, *33*, 5230−5237.
(12) Ren, X. L.; Tu, C. K.; Laipis, P. J.; Silverman, D. N. *Biochemistry* **1995**, *34*, 8492−8498.
(13) Knapp, M. J.; Rickert, K. W.; Klinman, J. P. *J. Am. Chem. Soc.* **2002**, *124*, 3865−3874.
(14) Mayer, J. M.; Hrovat, D. A.; Thomas, J. L.; Borden, W. T. *J. Am. Chem. Soc.* **2002**, *124*, 11142−11147.
(15) Hammes-Schiffer, S. *Chem. Phys. Chem.* **2002**, *3*, 33−42.
(16) Hammes-Schiffer, S. *Acc. Chem. Res.* **2001**, *34*, 273−281.
(17) Cukier, R. I. *J. Phys. Chem. B* **2002**, *106*, 1746−1757.
(18) Binstead, R. A.; McGuire, M. E.; Dovletoglou, A.; Seok, W. K.; Roecker, L. E.; Meyer, T. J. *J. Am. Chem. Soc.* **1992**, *114*, 173−186.

at the transition state geometry. For the phenoxyl/phenol system, the SOMO is dominated by 2p orbitals on the donor and acceptor oxygen atoms that are perpendicular to the proton donor−acceptor (O···H···O) axis, while the proton participates in a hydrogen bond involving σ orbitals. Since the electron and proton are transferred between different sets of orbitals, the authors describe this reaction as PCET. For the benzyl/toluene system, the SOMO is dominated by atomic orbitals oriented along the donor−acceptor (C···H···C) axis, and the authors describe this reaction as HAT. This analysis serves as a useful way to distinguish between these two types of reactions. For convenience, we will use these definitions of HAT and PCET and will use the term "general PCET" to encompass all reactions involving electron and proton transfer in a single step. Note that the distinction between sequential and concerted transfer within this single step is not well defined because the electron and proton behave quantum mechanically.

In this paper, we present a different analysis of the phenoxyl/phenol and benzyl/toluene systems and gain additional insight into the fundamental differences between these two types of reactions. Since hydrogen tunneling is often important in these types of reactions, we treat the transferring hydrogen nucleus quantum mechanically and calculate the vibronic coupling between the mixed electronic−proton vibrational wavefunctions corresponding to the reactant and the product states. Even when the splitting between the ground and excited electronic states is much larger than the thermal energy, k_BT, these types of reactions are often vibronically nonadiabatic with respect to the solvent and protein environment because the vibronic coupling is much less than k_BT. In this case, the rate of the reaction is proportional to the square of the vibronic coupling.[19−22] As a result, the magnitude of the vibronic coupling and its dependence on the proton donor−acceptor distance can significantly impact the rates, kinetic isotope effects, and temperature dependences of general PCET reactions.[23,24] The impact of the vibronic coupling on the rates and kinetic isotope effects has been illustrated for PCET reactions in iron bi-imidazoline complexes,[25] oxoruthenium polypyridyl complexes,[26] ruthenium polypyridyl−tyrosine systems,[27] and the enzyme lipoxygenase.[28] Recently, the impact of the vibronic coupling on the temperature dependence of the kinetic isotope effect has been elucidated for the PCET reaction catalyzed by the enzyme lipoxygenase.[29] Thus, the calculation of the vibronic coupling is critical for a complete understanding of general PCET reactions.

In addition to calculating the vibronic coupling for these two systems, we identify a new diagnostic for differentiating between the two types of reactions. Our analysis utilizes the semiclassical analytical expression for the vibronic coupling derived by Georgievskii and Stuchebrukhov,[30] as well as analytical expressions in the limits of electronically adiabatic and nonadiabatic proton tunneling. Even when the overall reaction is vibronically nonadiabatic, the proton tunneling can be in the electronically adiabatic or electronically nonadiabatic limits or in the intermediate regime. Here the proton tunneling is defined to be electronically adiabatic when the electronic transition time is much shorter than the proton tunneling time, so the electrons are able to respond virtually instantaneously to the proton motion, and the reaction proceeds on the electronically adiabatic ground state. The proton tunneling is defined to be electronically nonadiabatic when the electronic transition time is much longer than the proton tunneling time, so the electrons are unable to rearrange fast enough to follow the proton motion, and the excited electronic state is involved in the reaction. Our analysis indicates that the phenoxyl/phenol reaction, which was previously identified to be PCET, is electronically nonadiabatic, while the benzyl/toluene reaction, which was previously identified to be HAT, is electronically adiabatic. These links between PCET and electronic nonadiabaticity and between HAT and electronic adiabaticity provide insights into the fundamental physical differences between these two types of reactions.

The paper is organized as follows. Section II presents the theoretical framework and the computational methodology. Section III presents the results and an extensive analysis. Conclusions are summarized in section IV.

II. Theory and Methods

A. Analytical Expressions for Vibronic Couplings. Previously we developed a theoretical formulation for general PCET reactions and derived vibronically nonadiabatic rate expressions.[19,20,31] In this formulation, the PCET reaction occurs between two diabatic electronic states, denoted I and II, representing the localized electron transfer states. The transferring electron is localized on the donor for diabatic state I and on the acceptor for diabatic state II. The proton vibrational wavefunctions are calculated for each diabatic electronic state, leading to a set of reactant and product proton vibrational wavefunctions denoted $\varphi_D^{(I)}$ and $\varphi_A^{(II)}$, respectively. For simplicity, here we consider the tunneling between only the ground state reactant and product mixed electronic−proton vibrational states. In this case, the rate of reaction is proportional to the square of the vibronic coupling, which is defined to be the Hamiltonian matrix element between the reactant and product mixed electronic−proton vibrational wavefunctions. The overall reaction is vibronically nonadiabatic with respect to the solvent or protein environment when this vibronic coupling is much less than k_BT. As mentioned above, even for vibronically nonadiabatic PCET reactions, the proton tunneling can be electronically nonadiabatic, electronically adiabatic, or in the intermediate regime. Our previously derived rate expressions for general PCET reactions are valid in all of these regimes.[19,20]

In this paper, the electronically nonadiabatic and adiabatic limits for general PCET reactions refer to the relative time scales of the electrons and the transferring proton. The electrons

(19) Soudackov, A.; Hammes-Schiffer, S. *J. Chem. Phys.* **2000**, *113*, 2385−2396.
(20) Soudackov, A.; Hatcher, E.; Hammes-Schiffer, S. *J. Chem. Phys.* **2005**, *122*, 014505.
(21) Cukier, R. I. *J. Phys. Chem.* **1996**, *100*, 15428−15443.
(22) Cukier, R. I.; Nocera, D. G. *Annu. Rev. Phys. Chem.* **1998**, *49*, 337−369.
(23) Hammes-Schiffer, S.; Iordanova, N. *Biochim. Biophys. Acta−Bioenergetics* **2004**, *1655*, 29−36.
(24) Hatcher, E.; Soudackov, A.; Hammes-Schiffer, S. *J. Phys. Chem. B* **2005**, *109*, 18565−18574.
(25) Iordanova, N.; Decornez, H.; Hammes-Schiffer, S. *J. Am. Chem. Soc.* **2001**, *123*, 3723−3733.
(26) Iordanova, N.; Hammes-Schiffer, S. *J. Am. Chem. Soc.* **2002**, *124*, 4848−4856.
(27) Carra, C.; Iordanova, N.; Hammes-Schiffer, S. *J. Am. Chem. Soc.* **2003**, *125*, 10429−10436.
(28) Hatcher, E.; Soudackov, A. V.; Hammes-Schiffer, S. *J. Am. Chem. Soc.* **2004**, *126*, 5763−5775.
(29) Hatcher, E.; Soudackov, A. V.; Hammes-Schiffer, S. *J. Am. Chem. Soc.*, in press.
(30) Georgievskii, Y.; Stuchebrukhov, A. A. *J. Chem. Phys.* **2000**, *113*, 10438−10450.
(31) Soudackov, A.; Hammes-Schiffer, S. *J. Chem. Phys.* **1999**, *111*, 4672−4687.

respond instantaneously to the proton motion in the electronically adiabatic limit but not in the electronically nonadiabatic limit. In the electronically nonadiabatic limit, the vibronic coupling $V_{DA}^{(na)}$ can be expressed as the product of the electronic coupling and the Franck−Condon overlap of the reactant and product proton vibrational wavefunctions:

$$V_{DA}^{(na)} = V^{ET}\langle\varphi_D^{(I)}|\varphi_A^{(II)}\rangle \quad (1)$$

In the electronically adiabatic limit, the proton dynamics occur on the electronically adiabatic ground state potential energy surface, and the vibronic coupling $V_{DA}^{(ad)}$ can be calculated by standard semiclassical methods.[32,33] For a symmetric system, the vibronic coupling $V_{DA}^{(ad)}$ is half the splitting between the symmetric and antisymmetric proton vibrational states for the electronic ground state potential energy surface.

Many general PCET reactions are in between the electronically nonadiabatic and adiabatic limits. Georgievskii and Stuchebrukhov[30] derived a semiclassical expression for the general vibronic coupling, $V_{DA}^{(sc)}$:

$$V_{DA}^{(sc)} = \kappa V_{DA}^{(ad)} \quad (2)$$

where the factor κ is defined as

$$\kappa = \sqrt{2\pi p}\,\frac{e^{p\ln p - p}}{\Gamma(p+1)} \quad (3)$$

In eq 3, $\Gamma(x)$ is the gamma function and p is the proton adiabaticity parameter, defined as

$$p = \frac{|V^{ET}|^2}{\hbar|\Delta F|v_t} \quad (4)$$

where v_t is the tunneling velocity of the proton at the crossing point of the two proton potential energy curves and $|\Delta F|$ is the difference between the slopes of the proton potential energy curves at the crossing point. The tunneling velocity v_t can be expressed in terms of the energy V_c at which the potential energy curves cross, the tunneling energy E, and the mass m of the proton:

$$v_t = \sqrt{\frac{2(V_c - E)}{m}} \quad (5)$$

In the electronically adiabatic limit, $p \gg 1$, $\kappa = 1$, and the vibronic coupling simplifies to $V_{DA}^{(ad)}$. In the electronically nonadiabatic limit, $p \ll 1$, $\kappa = (2\pi p)^{1/2}$, and the vibronic coupling reduces to $V_{DA}^{(na)}$, as given in eq 1.

The adiabaticity of a general PCET reaction can be viewed in terms of the relative times of the proton tunneling and the electronic transition. Within the semiclassical framework, the time spent by the tunneling proton in the crossing region (i.e., the proton tunneling time) is

$$\tau_p \sim \frac{V^{ET}}{|\Delta F|v_t} \quad (6)$$

and the time required to change the electronic state (i.e., the electronic transition time) is

$$\tau_e \sim \frac{\hbar}{V^{ET}} \quad (7)$$

The adiabaticity parameter is simply the ratio of these two times:

$$p = \frac{\tau_p}{\tau_e} \quad (8)$$

When the proton tunneling time is much longer than the electronic transition time, the electronic states have enough time to mix completely and the proton transfer occurs on the electronically adiabatic ground state surface (i.e., the reaction is electronically adiabatic). When the proton tunneling time is much less than the electronic transition time, the reaction is electronically nonadiabatic because the electronic states no longer have enough time to mix completely during the proton tunneling process.

B. Computational Methodology. We calculated the input quantities for the vibronic coupling expressions with conventional electronic structure methods. We emphasize that our goal is not to provide quantitatively accurate results for these specific systems, but rather to enable a qualitative comparison of the fundamental nature of these two types of systems. As a result, we utilize moderate levels of electronic structure theory that provide physically reasonable results. The quantitative accuracy of the results can be improved by using a larger basis set and including dynamical electron correlation. Unless otherwise specified, we used the Gaussian03 package[34] for these electronic structure calculations.

We obtained the transition state geometries, which were optimized with density functional theory (DFT) using the B3LYP functional[35,36] and the 6-31G* basis set,[37] from ref 14. The qualitative dependence of the vibronic coupling on the donor−acceptor distance was determined by translating the rigid donor and acceptor molecules along the donor−acceptor axis for the transition state geometry. For each donor−acceptor distance, all nuclei were fixed except for the transferring hydrogen, which was treated quantum mechanically. In this paper, the reactant and product states refer to the mixed electronic−proton vibrational quantum states in which the electron and proton are localized on the donor in the reactant state and on the acceptor in the product state for fixed geometry of all other nuclei. In general, the Franck−Condon overlap factor from the other nuclei could contribute to the vibronic coupling, but this contribution is not directly relevant to the analysis presented in this paper.

We obtained the electronically adiabatic ground and excited state potential energy curves along the hydrogen coordinate by calculating the state-averaged CASSCF(3,6) energy for the hydrogen positioned at discrete grid points along the axis connecting the donor and acceptor atoms. The active space was chosen to ensure that the character of the orbitals in the active space was conserved along the hydrogen coordinate and the

(32) Vorotyntsev, M. A.; Dogonadze, R. R.; Kuznetsov, A. M. *Dokl. Akad. Nauk SSSR* **1973**, *209*, 1135.
(33) Fain, B. *Theory of Rate Processes in Condensed Media*; Springer: New York, 1980.
(34) Frisch, M. J.; et al. *Gaussian 03*, revision C.03; Gaussian, Inc.: Pittsburgh, PA, 2003.
(35) Lee, C.; Yang, W.; Parr, P. G. *Phys. Rev. B* **1988**, *37*, 785−789.
(36) Becke, A. D. *J. Chem. Phys.* **1993**, *98*, 5648−5652.
(37) Hariharan, P. C.; Pople, J. A. *Theor. Chim. Acta* **1973**, *28*, 213−222.

electronic ground state was qualitatively similar to the ROHF ground state. As discussed below, we also calculated three-dimensional potential energy surfaces for the hydrogen at the ROHF level. The 6-31G basis set[38] was used for all ROHF and CASSCF calculations to enable the efficient calculation of the three-dimensional potential energy surfaces. We determined that the ground and excited state potential energy surfaces are qualitatively similar for the 6-31G and 6-31G* basis sets.

The quantities in the expressions for the vibronic couplings given in section IIA were determined from the CASSCF potential energy curves. The electronic coupling V^{ET} is half the splitting between the two electronically adiabatic CASSCF potential energy curves at the midpoint between the donor and acceptor atoms. A two-state valence bond model was used to fit the state-averaged CASSCF potential energy curves for the purpose of obtaining the two localized electronically diabatic potential energy curves for the phenoxyl/phenol system. A four-state valence bond model was used for the benzyl/toluene system. The details of both of these valence bond models are given in the Supporting Information. The quantities $|\Delta F|$ and V_c in eqs 4 and 5, respectively, were determined from these electronically diabatic potential energy curves. The one-dimensional hydrogen vibrational wavefunctions were calculated for the diabatic and adiabatic potential energy curves using the Fourier grid Hamiltonian method[39,40] with 128 grid points. The Franck−Condon overlap in eq 1 is the overlap between the proton vibrational wavefunctions for the two diabatic potential energy curves. The electronically adiabatic vibronic coupling $V_{DA}^{(ad)}$ is half the splitting between the ground and excited hydrogen vibrational states for the electronically adiabatic ground state potential energy curve. The tunneling energy E in eq 5 is the hydrogen vibrational ground state energy for the electronically diabatic potential energy curve.

To study the impact of the three-dimensional character of the hydrogen vibrational wavefunction, we also calculated three-dimensional potential energy surfaces for the hydrogen at the ROHF level. For the electronically nonadiabatic system, we obtained the electronically diabatic potential energy curves by calculating the ROHF energy for a three-dimensional grid with 32 grid points per dimension spanning half of the proton donor−acceptor axis, fitting the data points to an analytical functional form (i.e., a fourth-order polynomial), and using the analytical functional form to generate the potential energy surface for a grid with 64 points per dimension. For the electronically adiabatic system, we obtained the electronically adiabatic ground state potential energy surface by calculating the ROHF energy for a three-dimensional grid with 32 points per dimension. The three-dimensional hydrogen vibrational wavefunctions were calculated for the ROHF potential energy surfaces using the Fourier grid Hamiltonian method.[39,40] We used the GAMESS electronic structure program[41] for the three-dimensional calculations.

This analysis has two main practical advantages over the orbital-based analysis in ref 14. First, the present analysis may be more reliable because the molecular orbitals corresponding to the electronically adiabatic ground state at the transition state geometry may not be meaningful for electronically nonadiabatic reactions. Second, the present analysis provides the vibronic couplings, which are required for calculating rates and kinetic isotope effects.

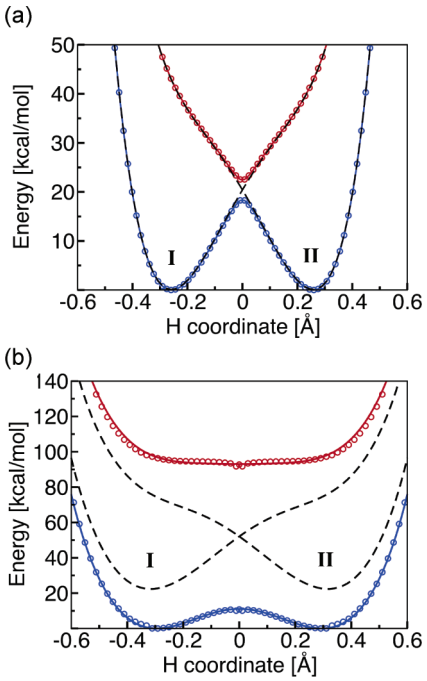

Figure 1. State-averaged CASSCF ground and excited state electronically adiabatic potential energy curves along the transferring hydrogen coordinate for (a) the phenoxyl/phenol system and (b) the benzyl/toluene system. The coordinates of all nuclei except the transferring hydrogen correspond to the transition state geometry. The proton donor−acceptor distances are 2.40 and 2.72 Å, respectively, for the phenoxyl/phenol and the benzyl/ toluene system. The CASSCF results are depicted as open circles that are blue for the ground state and red for the excited state. The black dashed lines represent the diabatic potential energy curves corresponding to the two localized diabatic electron transfer states I and II. The mixing of these two diabatic states with the electronic coupling V^{ET} leads to the CASSCF ground and excited state electronically adiabatic curves depicted with solid colored lines following the colored open circles. For the phenoxyl/phenol system, the solid colored lines and the black dashed lines are nearly indistinguishable because the adiabatic and diabatic potential energy curves are virtually identical except in the transition state region.

III. Results

As discussed previously, the transition state geometries of the phenoxyl/phenol and the benzyl/toluene systems are qualitatively different. The phenoxyl/phenol transition state has C_2 symmetry, and the O···H···O bond is approximately planar with the phenol rings. The proton donor−acceptor distance is 2.40 Å, and the system forms a strong hydrogen bond along the O···H···O axis. The benzyl/toluene transition state has C_{2h} symmetry, and the C···H···C bond is orthogonal to the planes of the benzene rings. The proton donor−acceptor distance is 2.72 Å, and the system does not form a strong hydrogen bond along the C···H···C axis because of the lack of lone pairs of electrons on benzyl and toluene.

Figure 1 depicts the potential energy curves along the transferring hydrogen coordinate for the phenoxyl/phenol and the benzyl/toluene systems. The CASSCF electronically adiabatic ground and excited state curves are depicted. The electronically diabatic curves corresponding to the two electron

(38) Hehre, W. J.; Ditchfield, R.; Pople, J. A. *J. Chem. Phys.* **1972**, *56*, 2257−2261.
(39) Webb, S. P.; Hammes-Schiffer, S. *J. Chem. Phys.* **2000**, *113*, 5214−5227.
(40) Marston, C. C.; Balint-Kurti, G. G. *J. Chem. Phys.* **1989**, *91*, 3571.
(41) Schmidt, M. W.; Baldridge, K. K.; Boatz, J. A.; Elbert, S. T.; Gordon, M. S.; Jensen, J. H.; Koseki, S.; Matsunaga, N.; Nguyen, K. A.; Su, S.; Windus, T. L.; Dupuis, M.; Montgomery, J. A. *J. Comput. Chem.* **1993**, *14*, 1347−1363.

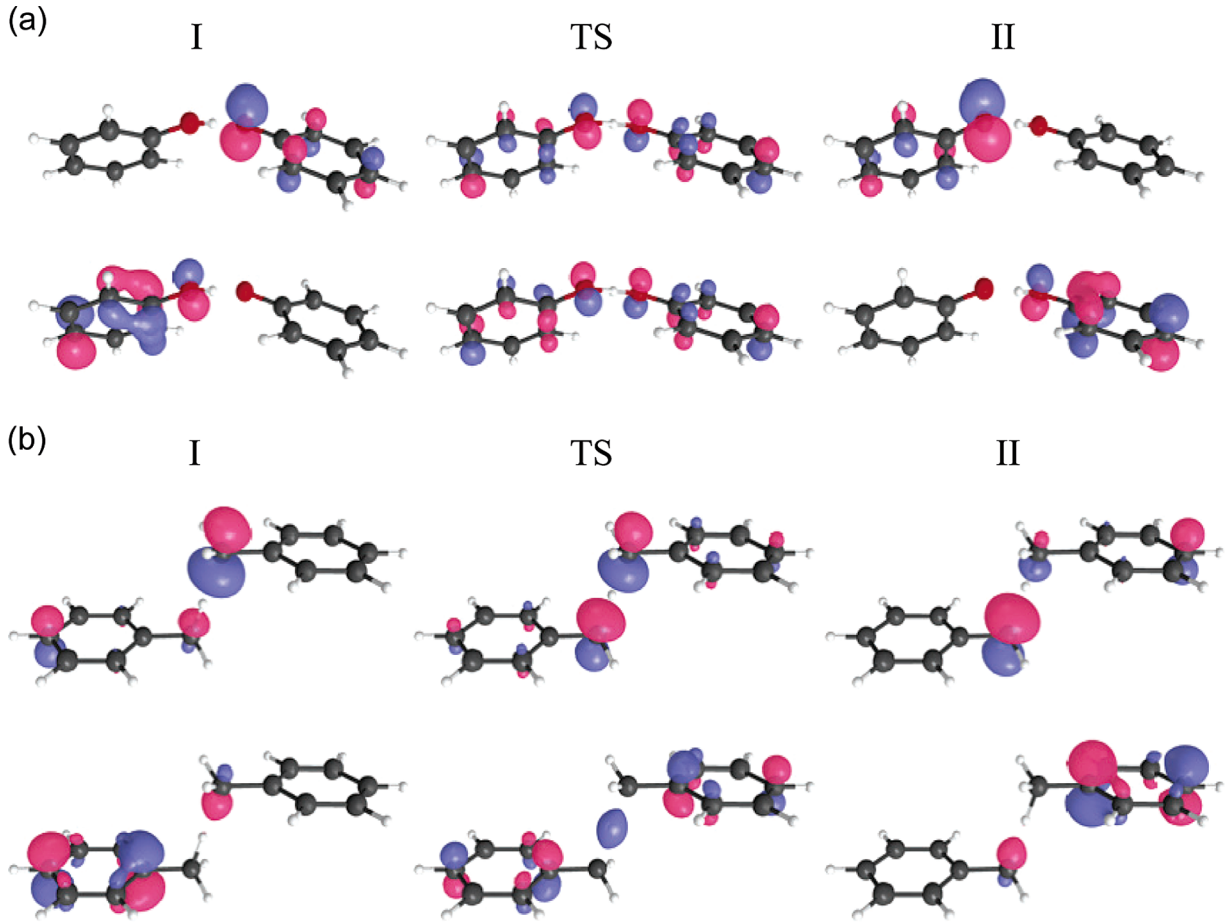

Figure 2. The two highest-energy occupied electronic molecular orbitals for (a) the phenoxyl/phenol system and (b) the benzyl/toluene system. The electronic wavefunctions for diabatic states I and II are calculated at the minima of the ground state electronically adiabatic potential energy curves shown in Figure 1, and the electronic wavefunctions for the transition states (TS) are calculated at the maxima of these potential energy curves. For both systems, the ground state electronic wavefunction is predominantly single configurational, and the lower molecular orbital is doubly occupied, while the upper molecular orbital is singly occupied. These figures were generated with MacMolPlot.[46]

transfer states, denoted I and II, are also depicted. These diabatic states correspond to fixed electronic wavefunctions associated with the hydrogen bonded to the donor atom (I) or to the acceptor atom (II). By construction, the mixing of these two diabatic states with the appropriate coupling V^{ET} leads to the CASSCF electronically adiabatic ground and excited state curves. Note that the splitting between the electronically adiabatic ground and excited states is more than an order of magnitude larger for the benzyl/toluene system than for the phenoxyl/phenol system. As a result, the diabatic curves are very similar to the adiabatic curves for the phenoxyl/phenol system but are significantly different from the adiabatic curves for the benzyl/toluene system.

The two highest-energy occupied electronic molecular orbitals are depicted in Figure 2 for the phenoxyl/phenol and the benzyl/toluene systems. The diabatic states I and II are represented by the electronic wavefunctions corresponding to the minima of the potential energy curves. For both systems, the ground state electronic wavefunction is predominantly single configurational in the regions near the minima. For diabatic state I, the highest doubly occupied molecular orbital is localized mainly on the conjugated π system of the donor ring, and the singly occupied molecular orbital is localized mainly on the acceptor oxygen or carbon. The opposite configuration is observed for diabatic state II. For both systems, the electron transfer process is represented by the change in the electronic wavefunction as the system proceeds from diabatic state I to diabatic state II. The change in the electronic wavefunction involves the shifting of electronic density of the doubly occupied molecular orbital from the conjugated π orbital on the donor ring to the conjugated π orbital on the acceptor ring, as well as the shifting of electronic density of the singly occupied molecular orbital from the acceptor oxygen or carbon to the donor oxygen or carbon.

The electronic wavefunctions for the two systems are qualitatively different at the transition state. For both systems, the ground state electronic wavefunction remains predominantly single configurational at the transition state. In the phenoxyl/phenol system, the two highest-energy occupied molecular orbitals are dominated by 2p orbitals on the donor and acceptor oxygen atoms that are perpendicular to the hydrogen donor−acceptor axis. In the ground state, the doubly occupied molecular orbital corresponds to π-bonding, and the singly occupied molecular orbital corresponds to π-antibonding. In the benzyl/toluene system, the two highest-energy occupied molecular orbitals are dominated by σ orbitals on the donor and acceptor carbon atoms and are oriented along the hydrogen donor−acceptor axis. In the ground state, the highest doubly occupied molecular orbital corresponds to σ-bonding, and the singly occupied molecular orbital corresponds to σ-antibonding. Previously Mayer, Borden, and co-workers[14] used these differences in the singly occupied molecular orbitals of the transition state

Table 1. Electronic Coupling V^{ET}, Adiabaticity Parameter p, Prefactor κ, Proton Tunneling Time τ_p, and Electronic Transition Time τ_e for the Phenoxyl/Phenol and Benzyl/Toluene Systems

system[a]	V^{ET} (cm^{-1})	p	κ	τ_p (fs)	τ_e (fs)
phenol	700	0.0130	0.268	0.098	7.60
toluene	14 300	3.45	0.976	1.28	0.370

[a] The proton donor−acceptor distances are 2.40 and 2.72 Å, respectively, for the phenoxyl/phenol and benzyl/toluene systems.

Table 2. Vibronic Couplings in cm^{-1} for the Phenoxyl/Phenol System, Calculated with the Semiclassical Method ($V_{DA}^{(sc)}$) and for the Adiabatic ($V_{DA}^{(ad)}$) and Nonadiabatic ($V_{DA}^{(na)}$) Limits[a]

	hydrogen			deuterium		
R_{oo} (Å)	$V_{DA}^{(ad)}$	$V_{DA}^{(sc)}$	$V_{DA}^{(na)}$	$V_{DA}^{(ad)}$	$V_{DA}^{(sc)}$	$V_{DA}^{(na)}$
2.25	198	78.2	72.9	47.2	20.6	18.7
2.30	104	35.8	33.4 (15.3)	17.1	6.61	6.08 (2.59)
2.35	46.7	14.5	13.7 (7.23)	5.04	1.77	1.65 (0.90)
2.40	17.3	4.65	4.47 (2.86)	1.11	0.34	0.33 (0.25)
2.45	6.10	1.49	1.45 (1.11)	0.23	0.07	0.06 (0.06)
2.50	1.96	0.42	0.41 (0.36)	0.04	0.01	0.01 (0.01)

[a] The values in parentheses are the vibronic couplings calculated with the transferring hydrogen nucleus represented by a three-dimensional vibrational wavefunction. For all other values of the vibronic coupling given, the transferring hydrogen nucleus is represented by a one-dimensional vibrational wavefunction. The vibronic couplings are given for both hydrogen and deuterium transfer.

wavefunctions to designate the phenoxyl/phenol and benzyl/tolune systems as PCET and HAT, respectively.

Table 1 presents the electronic coupling V^{ET}, the adiabaticity parameter p, the prefactor κ, the proton tunneling time τ_p, and the electronic transition time τ_e for the two reactions. For both systems, the electronic coupling is significantly greater than the thermal energy k_BT at room temperature. As will be shown below, however, the overall vibronic coupling is significantly less than k_BT, leading to an overall vibronically nonadiabatic reaction with respect to a solvent environment at room temperature for both systems. The remainder of this analysis focuses on the electronic adiabaticity and nonadiabaticity of the proton tunneling process.

The fundamental nature of the proton tunneling is different for the two systems. For the phenoxyl/phenol system, the adiabaticity parameter p is very small, $\kappa \approx (2\pi p)^{1/2}$, and $\tau_e \approx 80\tau_p$. In this case, the electronic transition time is significantly greater than the proton tunneling time. As a result, the electrons are not able to rearrange fast enough for the proton to move on the electronically adiabatic ground state surface, and the proton transfer reaction is electronically nonadiabatic. For the benzyl/toluene system, the adiabaticity parameter p is larger, $\kappa \approx 1$, and $\tau_p \approx 4\tau_e$. In this case, the electronic transition time is less than the proton tunneling time. Thus, the electrons can respond instantaneously to the proton motion, and the proton moves on the electronically adiabatic ground state surface. This analysis indicates that the proton tunneling is electronically nonadiabatic for the phenoxyl/phenol system but electronically adiabatic for the benzyl/toluene system.

The vibronic couplings calculated with the adiabatic, nonadiabatic, and semiclassical methods are provided in Tables 2 and 3 for the phenoxyl/phenol and benzyl/toluene systems, respectively. In all cases, the adiabatic vibronic couplings are larger than the nonadiabatic vibronic couplings. The semiclassical vibronic couplings are in excellent agreement with the

Table 3. Vibronic Couplings in cm^{-1} for the Benzyl/Toluene System Calculated with the Semiclassical Method ($V_{DA}^{(sc)}$) and for the Adiabatic ($V_{DA}^{(ad)}$) and Nonadiabatic ($V_{DA}^{(na)}$) Limits[a]

	hydrogen			deuterium		
R_{oo} (Å)	$V_{DA}^{(ad)}$	$V_{DA}^{(sc)}$	$V_{DA}^{(na)}$	$V_{DA}^{(ad)}$	$V_{DA}^{(sc)}$	$V_{DA}^{(na)}$
2.60	167 (116)	163	58.7	42.5 (26.0)	41.8	4.07
2.65	87.8 (57.0)	85.8	25.4	14.9 (8.43)	14.5	1.23
2.70	38.5 (24.8)	37.5	10.8	4.06 (2.38)	3.99	0.37
2.72	21.6 (16.1)	21.1	5.58	1.70 (1.25)	1.67	0.14
2.75	15.0 (9.89)	14.6	3.96	0.97 (0.61)	0.95	0.08
2.80	7.36 (3.64)	7.16	2.36	0.35 (0.14)	0.34	0.04

[a] The values in parentheses are the vibronic couplings calculated with the transferring hydrogen nucleus represented by a three-dimensional vibrational wavefunction. For all other values of the vibronic coupling given, the transferring hydrogen nucleus is represented by a one-dimensional vibrational wavefunction. The vibronic couplings are given for both hydrogen and deuterium transfer.

nonadiabatic couplings for the phenoxyl/phenol system and are in excellent agreement with the adiabatic couplings for the benzyl/toluene system. These results confirm that the proton transfer is electronically nonadiabatic for the phenoxyl/phenol reaction and electronically adiabatic for the benzyl/toluene reaction. Tables 2 and 3 also provide the vibronic couplings for the deuterated phenoxyl/phenol and benzyl/toluene systems, respectively. For a given proton donor−acceptor distance, the vibronic couplings are significantly smaller for deuterium than for hydrogen because of the greater localization of the deuterium wavefunction, leading to smaller overlaps between the reactant and product proton vibrational wavefunctions.

Figure 3 illustrates the physical principles underlying the electronically nonadiabatic and adiabatic limits. For the electronically nonadiabatic phenoxyl/phenol reaction, the vibronic coupling is the product of the electronic coupling between the diabatic states I and II and the overlap of the reactant and product proton vibrational wavefunctions corresponding to these diabatic states. For the electronically adiabatic benzyl/toluene reaction, the vibronic coupling is half the energy splitting between the states corresponding to the symmetric and antisymmetric proton vibrational wavefunctions for the electronically adiabatic ground state.

The distance dependence of the vibronic coupling plays a key role in determining the rates and kinetic isotope effects, as well as the temperature dependences, of general PCET reactions. The dependence of the vibronic couplings on the proton donor−acceptor distance is depicted in Figure 4 for the two systems. In the electronically nonadiabatic limit, this distance dependence is dominated by the overlap between the reactant and product proton vibrational wavefunctions. As shown in ref 44, in the region close to the equilibrium value $\bar{R}$, the overlap can be approximated to be of the form $S(R) \propto S(\bar{R}) \exp[-\alpha(R - \bar{R})]$. In the electronically adiabatic limit, the semiclassical tunneling matrix element for proton transfer can also be approximated to depend exponentially on the proton donor−acceptor distance.[42,43] Thus, our recent theoretical treatment of general PCET reactions assumes an exponential dependence of the vibronic coupling on the proton donor−acceptor distance:[20,24,44]

(42) Borgis, D.; Hynes, J. T. *Chem. Phys.* **1993**, *170*, 315−346.
(43) Kiefer, P. M.; Hynes, J. T. *Solid State Ionics* **2004**, *168*, 219.
(44) Hatcher, E.; Soudackov, A.; Hammes-Schiffer, S. *Chem. Phys.* **2005**, *319*, 93−100.

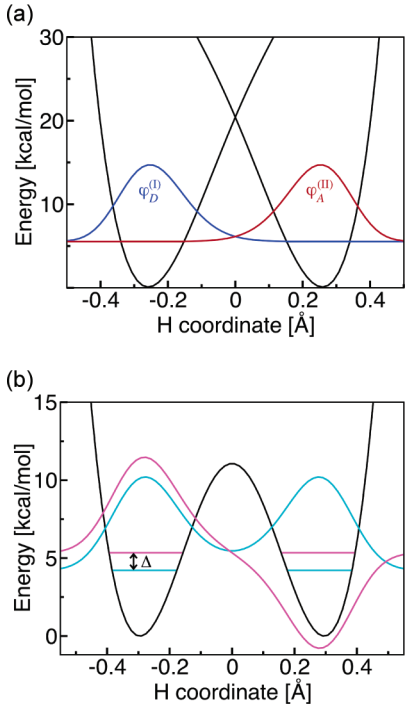

Figure 3. (a) Diabatic potential energy curves corresponding to the two localized diabatic electron transfer states I and II and the corresponding proton vibrational wavefunctions $\varphi_D^{(I)}$ (blue) and $\varphi_A^{(II)}$ (red) for the phenoxyl/phenol system. Since this reaction is electronically nonadiabatic, the vibronic coupling is the product of the electronic coupling V^{ET} and the overlap of the reactant and product proton vibrational wavefunctions $\langle\varphi_D^{(I)}|\varphi_A^{(II)}\rangle$. (b) Electronically adiabatic ground state potential energy curve and the corresponding proton vibrational wavefunctions for the benzyl/toluene system. Since this reaction is electronically adiabatic, the vibronic coupling is equal to half of the energy splitting Δ between the symmetric (cyan) and antisymmetric (magenta) proton vibrational states for the electronic ground state potential energy surface. For illustrative purposes, the excited vibrational state is shifted up in energy by 0.8 kcal/mol.

$$V_{DA} = V_{DA}^{(0)} \exp[-\alpha(R - \bar{R})] \quad (9)$$

where $V_{DA}^{(0)}$ is the value of the vibronic coupling at the equilibrium distance $\bar{R}$. The results shown in Figure 4 validate the exponential dependence of the vibronic couplings on the proton donor−acceptor distance for both systems in the range of distances studied.

The values of α for both hydrogen and deuterium transfer for both systems are given in Table 4. The values of α are slightly larger for the phenoxyl/phenol system than for the benzyl/toluene system because of differences in the frequencies and energy barriers. For the phenoxyl/phenol system, which is electronically nonadiabatic, the value of α is dominated by the dependence of the overlap $\langle\varphi_D^{(I)}|\varphi_A^{(II)}\rangle$ on the proton donor−acceptor distance. The values of α are larger for deuterium than for hydrogen because the overlap between the reactant and product deuterium wavefunctions falls off faster with distance than the corresponding overlap for the hydrogen wavefunctions due to the larger mass of deuterium.

The vibronic couplings are reduced when the transferring hydrogen nucleus is represented by a three-dimensional rather than a one-dimensional vibrational wavefunction. The extensions of the electronically nonadiabatic and adiabatic limits to three dimensions are straightforward. In the electronically nonadiabatic limit, we calculated the three-dimensional potential energy surface for the two diabatic states at the ROHF level and

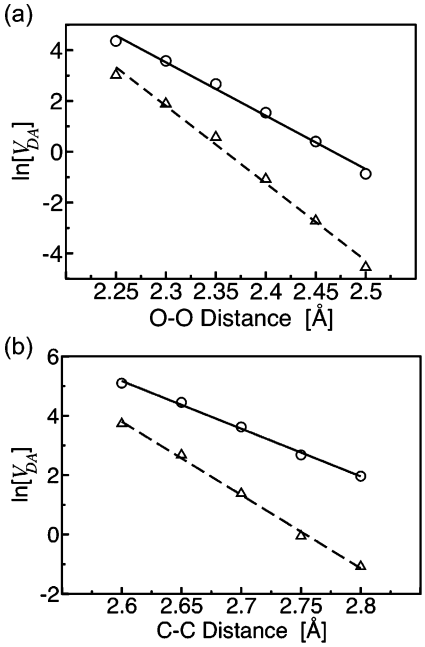

Figure 4. Dependence of the semiclassical vibronic couplings $V_{DA}^{(sc)}$ on the proton donor−acceptor distance R for (a) the phenoxyl/phenol system and (b) the benzyl/toluene system. The results for hydrogen transfer are shown as open circles, and the results for deuterium transfer are shown as open triangles. The dashed and solid lines correspond to a fit to the functional form $\exp[-\alpha R]$ for hydrogen (solid) and deuterium (dashed) transfer. The corresponding values of α are given in Table 4. The couplings $V_{DA}^{(sc)}$ are in units of cm^{-1}.

Table 4. Values of α, the Dependence of the Vibronic Coupling on the Proton Donor−Acceptor Distance R, for the Phenoxyl/Phenol and Benzyl/Toluene Systems[a]

system	α (1D)	α (3D)
phenol (H)	20	19
phenol (D)	28	28
toluene (H)	15	17
toluene (D)	24	26

[a] The distance dependence of the vibronic coupling is fit to the functional form $\exp[-\alpha R]$. The α values are given for both the one-dimensional (1D) and three-dimensional (3D) treatment of hydrogen (H) and deuterium (D). The values of α are given in $Å^{-1}$.

calculated the overlap between the corresponding three-dimensional hydrogen vibrational wavefunctions. In the electronically adiabatic limit, we calculated the three-dimensional potential energy surface for the electronic ground state at the ROHF level and calculated the energy splitting between the three-dimensional ground and excited state hydrogen vibrational wavefunctions. The results are given in Tables 2 and 3 for both hydrogen and deuterium for the two systems. The three-dimensional treatment of the transferring hydrogen decreases the vibronic coupling by as much as a factor of 2 and slightly decreases the kinetic isotope effect on the magnitude of the vibronic coupling. As shown in Table 4, the three-dimensional treatment of the transferring hydrogen does not significantly alter the value of α, which reflects the exponential dependence of the vibronic coupling on the proton donor−acceptor distance.

An alternative method for calculating the vibronic couplings with a three-dimensional treatment of the transferring hydrogen nucleus is the nuclear−electronic orbital nonorthogonal configuration interaction (NEO-NOCI) method.[45] This method treats the electrons and transferring proton on equal footing with molecular orbital techniques and provides mixed nuclear−

electronic wavefunctions. Future work will explore the potential of the NEO-NOCI method for calculating vibronic couplings.

The magnitude and distance dependence of the vibronic coupling strongly impact the magnitudes and temperature dependences of the rates and kinetic isotope effects (KIEs). As derived previously[20,29] using a series of well-defined, physically reasonable approximations, the rate of a general PCET reaction can be expressed as

$$k = \sum_{\mu} P_{\mu} \sum_{\nu} \frac{|V_{\mu\nu}^{(0)}|^2}{\hbar} \exp\left[\frac{2k_B T \alpha_{\mu\nu}^2}{M\Omega^2}\right] \sqrt{\frac{\pi}{(\lambda + \lambda_\alpha)k_B T}} \times \exp\left[-\frac{(\Delta G^\circ + \lambda + \Delta\epsilon_{\mu\nu})^2}{4(\lambda + \lambda_\alpha)k_B T}\right] \quad (10)$$

where the summations are over reactant and product vibronic states, P_μ is the Boltzmann probability for the reactant state μ, λ is the solvent/protein reorganization energy, $\lambda_\alpha = \hbar^2\alpha_{\mu\nu}^2/2M$, ΔG° is the driving force, $\Delta\epsilon_{\mu\nu}$ is the difference between the product and reactant vibronic energy levels relative to the ground states, and M and Ω are the effective mass and frequency associated with the proton donor−acceptor motion. If we consider only the nonadiabatic transition between the two ground states, the KIE can be approximated as

$$\mathrm{KIE} \approx \frac{|V_H^{(0)}|^2}{|V_D^{(0)}|^2} \exp\left\{\frac{2k_B T}{M\Omega^2}(\alpha_H^2 - \alpha_D^2)\right\} \quad (11)$$

The temperature dependence of the KIE depends on the difference between the distance dependences of the vibronic couplings for hydrogen and deuterium. The magnitude of the KIE depends on this difference and on the ratio of the equilibrium vibronic couplings for hydrogen and deuterium. Thus, the calculation of the vibronic coupling is essential for predicting the magnitudes and temperature dependences of the rates and KIEs. Comparison of the calculated values to experimentally measured KIEs and their temperature dependences will be useful for validating this general approach and benchmarking the level of theory.

The distinction between electronic adiabaticity and nonadiabaticity has important experimental consequences because the vibronic couplings can be substantially different in the electronically adiabatic and nonadiabatic limits. These differences are clearly illustrated in Tables 2 and 3. As indicated by eqs 10 and 11, the magnitude and distance dependence of the vibronic coupling can significantly impact the magnitudes and temperature dependences of the rates and the KIEs. Thus, the calculation of the vibronic coupling in the correct limit, or in the intermediate regime, is critical for the interpretation of experimental data and the generation of experimentally testable predictions.

Furthermore, the experimentally measured magnitude and temperature dependence of the KIE may be useful in the classification of a reaction as electronically adiabatic (i.e., HAT mechanism) or electronically nonadiabatic (i.e., PCET mechanism). For complex systems, the calculation of the semiclassical vibronic coupling and the adiabaticity parameter may not be computationally practical. For these types of systems, the vibronic coupling could be calculated for the electronically adiabatic and electronically nonadiabatic limits, and the resulting values could be used in conjunction with eq 11 to estimate the magnitude and temperature dependence of the KIE. If the KIE is different in the two limits, a comparison to the experimental data could be used to determine the mechanism.

IV. Conclusions

In this paper, we calculated the vibronic couplings for the phenoxyl/phenol and the benzyl/toluene self-exchange reactions. The vibronic couplings significantly impact the rates and kinetic isotope effects, as well as the temperature dependences, of general PCET reactions. Although the splittings between the ground and excited electronic states are significantly larger than the thermal energy k_BT at room temperature, the vibronic couplings for both systems were found to be smaller than k_BT, indicating that the reactions are vibronically nonadiabatic with respect to a solvent environment. The proton tunneling was found to be electronically nonadiabatic for the phenoxyl/phenol system and electronically adiabatic for the benzyl/toluene system. For the phenoxyl/phenol system, the electronic transition time is significantly greater than the proton tunneling time. Thus, the electrons are not able to rearrange fast enough to follow the proton motion on the electronically adiabatic state, and the proton tunneling involves the excited electronic state. For the benzyl/toluene system, the electronic transition time is less than the proton tunneling time. As a result, the electrons can respond instantaneously to the proton motion, and the proton moves on the electronically adiabatic ground state surface.

We also examined the dependence of the vibronic coupling on the proton donor−acceptor distance and the deuterium kinetic isotope effect on both the magnitude and the distance dependence of the vibronic coupling. The vibronic coupling decreases exponentially with the proton donor−acceptor distance for both electronically adiabatic and electronically nonadiabatic reactions in the range of chemically relevant distances. For a given proton donor−acceptor distance, the vibronic couplings are significantly smaller for deuterium than for hydrogen because of the smaller overlap between the reactant and product proton vibrational wavefunctions for deuterium. Moreover, the value of the exponential decay parameter α is larger for deuterium than for hydrogen because the overlap between the reactant and product deuterium wavefunctions falls off faster with distance than the corresponding overlap for the hydrogen wavefunctions. Furthermore, the vibronic couplings are reduced but the value of α is not significantly altered when the transferring hydrogen nucleus is represented by a three-dimensional rather than a one-dimensional vibrational wavefunction. These trends are directly relevant to the study of general PCET reactions.

This type of analysis provides a new perspective on the distinction between PCET and HAT reactions. A conventional method for distinguishing PCET from HAT is that the electron and proton are transferred between different donors and acceptors (or different sets of orbitals) for PCET. Within this framework, our analysis suggests that PCET reactions are electronically nonadiabatic, whereas HAT reactions are electronically adiabatic. These two mechanisms can be differentiated by calculating the adiabaticity parameter, which depends on the electronic coupling and other quantities that can be determined

(45) Skone, J. H.; Pak, M. V.; Hammes-Schiffer, S. *J. Chem. Phys.* **2005**, *123*, 134108.
(46) Bode, B. M.; Gordon, M. S. *J. Mol. Graphics* **1998**, *16*, 133.

with quantum chemistry methods. Future work will be aimed at the classification of systems as PCET or HAT based on factors such as geometry and electronic structure.

Acknowledgment. We thank Mike Pak for helpful discussions regarding this work and Alexei Stuchebrukhov for bringing his paper to our attention. This work was supported by NSF grant CHE-05-01260, AFOSR grant F49550-04-1-0062, and NIH grant GM56207.

Supporting Information Available: Details for the valence bond models used to fit the CASSCF electronically adiabatic potential energy curves along the proton coordinate for the phenoxyl/phenol and the benzyl/toluene systems; complete ref 34. This material is available free of charge via the Internet at http://pubs.acs.org.

JA0656548